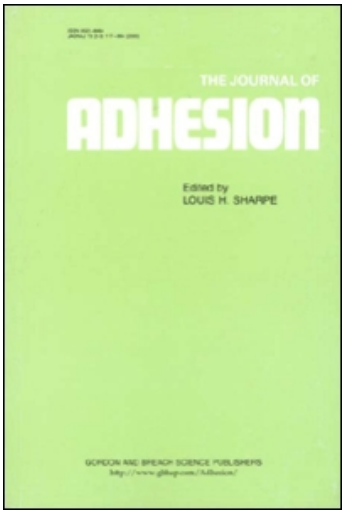

The Journal of Adhesion
Publication details, including instructions for authors and subscription information:
http://www.informaworld.com/smpp/title~content=t713453635

Two-Dimensional Analysis of Peeling Adhesive Tape from Human Skin

Raymond H. Plaut[a]
[a] Department of Civil and Environmental Engineering, Virginia Polytechnic Institute and State University, Blacksburg, Virginia, USA

Online publication date: 09 November 2010

To cite this Article Plaut, Raymond H.(2010) 'Two-Dimensional Analysis of Peeling Adhesive Tape from Human Skin', The Journal of Adhesion, 86: 11, 1086 — 1110
To link to this Article: DOI: 10.1080/00218464.2010.519257
URL: http://dx.doi.org/10.1080/00218464.2010.519257

The Journal of Adhesion, 86:1086–1110, 2010

ISSN: 0021-8464 print/1545-5823 online
DOI: 10.1080/00218464.2010.519257

Taylor & Francis
Taylor & Francis Group

Two-Dimensional Analysis of Peeling Adhesive Tape from Human Skin

Raymond H. Plaut
Department of Civil and Environmental Engineering, Virginia Polytechnic Institute and State University, Blacksburg, Virginia, USA

Adhesive tapes are attached to human skin for various purposes. When they are removed by peeling, discomfort or trauma may occur. Typically, the removed tape is partially covered by skin cells, and peeling involves failure within the substrate (skin), rather than just interfacial failure between the adhesive and the substrate, or cohesive failure within the adhesive. As an edge of the tape is pulled, first the skin deforms outward, and then peeling occurs after some threshold is attained. The literature is reviewed first, and then a two-dimensional analysis is developed. The tape is modeled as an extensible elastica, while the skin is represented as a nonlinear elastic strip with no bending stiffness. In the numerical results, the peel angle varies from 90° to 170°. Shapes of the tape and skin during pulling are determined, and the corresponding force is computed. For a certain peel criterion, the peel force is obtained.

Keywords: Deformable substrate; Peel force; Pressure-sensitive adhesive; Skin

1. INTRODUCTION

Medical products that involve adhesion to the skin include surgical tapes, first-aid bandages, transdermal drug delivery patches, and electrode attachments [1,2]. They must bond to the skin under a variety of conditions, such as flexure, changing temperature, perspiration, and external moisture. Then they should be easy to peel off, so that discomfort and trauma to the skin will be minimal. These conflicting characteristics need to be considered in the design of the adhesive and the backing to which it is attached.

Received 9 May 2010; in final form 6 July 2010.
Address correspondence to Raymond H. Plaut, Department of Civil and Environmental Engineering, MC 0105, Virginia Tech, Blacksburg, VA 24061, USA. E-mail: rplaut@vt.edu

Skin is a complex organ, and modeling its mechanical behavior is not simple. Its properties depend on age, gender, disease, obesity, body site, orientation, temperature, humidity, topical treatments, sun exposure, previous physical stress, and other factors [3,4]. When stretched, skin deforms easily at first but then becomes stiff. When plucked outward, as in peeling, there is resistance from the surrounding skin and from the tissue underneath. During peeling, ridges emanate outward from the peel front. Photographs of peeling from skin are presented in [5–9].

Discomfort and trauma caused by peeling tape from human skin have been correlated with the force used to pull the medical product from the skin in [6,10], but cases with poor correlation were described in [11–13]. The peel force depends on the peel angle and peel rate, in addition to the properties of the skin, adhesive, and backing. Based on experiments conducted at Virginia Tech [5,14,15], the peel force tends to increase as the peel rate increases (but naturally the duration of the peel process is reduced). Furyk *et al.* [16] presented test results showing that subjects tended to report lower pain when pressure-sensitive adhesive bandages were pulled at a high speed compared with slow removal over a 2-second period.

2. LITERATURE REVIEW

2.1. Human Skin

Human skin is comprised of solid and fluid components. It is usually described in terms of multiple layers, although the boundaries between the layers are not always distinct. The outermost layer is the stratum corneum (horny layer), which is composed of from three to over 50 layers of disk-shaped dead cells (corneocytes) bound together by intercellular lipids and degraded desmosomal protein junctions (corneodesmosomes) [17–21]. Cells may remain in the stratum corneum for 2 weeks [22]. It is the stiffest layer, but its thickness is only 0.010–0.015 mm over most of the body [23].

The stratum corneum is often included with the epidermis, which is 0.07–0.12 mm thick in most places [24]. The basement membrane separates the epidermis from the dermis. This membrane is wavy and has finger-like projections into the dermis [24]. The dermis is 1–5 mm thick and is sometimes divided into the papillary dermis and the reticular dermis [23,25]. It is the most important layer with regard to carrying forces, due to its elastin and collagen fibers [26]. Elastin fibers tend to furnish the most resistance to small forces. As the forces increase, the collagen fibers tend to straighten and provide

an increased resistance to deformation [27]. A layer of subcutaneous tissue, 0.4–4.0 mm thick, connects the dermis with the deep fascia (dense fibrous tissue) or underlying bonds [24,25]. Fibrous connecting strands allow the skin to have mobility and to glide parallel to its surface. Sometimes the skin becomes undermined, *i.e.*, separates from the subcutaneous tissue.

Skin is under passive tension in its rest state. Various "lines" of tension have been defined, such as Langer's lines, Kraissl's lines, Straiths's lines, and Bulacio's lines [28]. Gravity affects the tension in some parts of the body.

Many *in vivo* measurements of skin properties have been reported. The tests have involved tension, torsion, suction, and indentation [29,30]. As far as the author can ascertain, tests on the relationship between bending moment and curvature of the skin (either outward or inward) have not been reported in the literature. Such data would be useful in modeling the peeling of tape from skin.

A recent paper describing tests on skin tension is [31]. A multiaxial testing rig was applied to the skin surface on the volar forearm. The rig essentially pulled the skin radially with a circular attachment. The resulting stress-strain relationships for four subjects were almost bilinear, with an initial modulus of elasticity, E, around 50 kPa and a final value around 500 kPa. The transition occurred at strains in the range of 0.3–0.65. (In Figs. 5 and 6 of [31], the unit of stress should be kPa.)

Suction tests typically involve a guard ring with a diameter of 2–10 mm. The skin within the ring is displaced outward by a vacuum. Outward displacements are typically less than 1 mm, lower than in most cases of peeling that are of interest here. Standard devices are the Cutometer® and Dermaflex® [32,33].

Indentation tests have been described in a number of papers, including [34–38]. A rigid probe (indenter), usually spherical but sometimes conical, is pushed into the skin. The initial normal stiffness (*i.e.*, force divided by inward displacement) is often in the range of 10–25 N/m, and increases as the displacement increases (*i.e.*, the relationship is hardening).

2.2. Cohesive Forces in Stratum Corneum

According to Pailler-Mattei *et al.* [39], the corneocytes are about 500 nm thick and 40–50 μm in diameter, and are held together by an intercellular lipid matrix. Horstmann *et al.* [40] demonstrated how an adhesive can pull the outer layer of cells of the stratum corneum (and perhaps a few cells from the next layer) off the skin.

The inter-corneocyte cohesive forces tend to increase as one moves into the stratum corneum [41,42].

An instrument called a cohesograph was developed to measure these forces [43,44]. A circular metal disk with a diameter of 8 mm was adhered to the skin surface and then pulled outward. The adhesive penetrated two to three cell layers, and four to six layers of cells were removed by the procedure. The mean force was 0.9 N on the forearm, 1.1 N on the wrist, and 0.8 N on the back, with large standard deviations. As the process was repeated and more layers of the stratum corneum were removed, the force increased until it was approximately double its initial value.

Tests involving propagating cracks of *in vitro* samples of stratum corneum have been conducted to examine the fracture behavior. Koutroupi and Barbenel [17] used a shear specimen with a transverse crack and obtained a mean fracture energy of $3\,J/m^2$. Results of double-cantilever beam tests were reported by Wu *et al.* [45,46] and Levi *et al.* [47]. The beams were made of polycarbonate and bonded with a layer of stratum corneum. The critical delamination energy was measured in the range of $1–8\,J/m^2$, with the value dependent on the hydration, temperature, and chemical treatment of the layer.

2.3. Peeling Tape from Human Skin

Reported tests involving peeling from human skin *in vivo* will be described now. In some of the tests, tape is peeled from the skin multiple times at the same location (tape stripping or skin stripping). Each removal of tape may take a layer or more of cells off the stratum corneum, and tape stripping is sometimes used to determine how topically applied substances penetrate into the skin. It is also utilized to study the physiology of the stratum corneum, epidermal wound healing, and excretion of endogenous substances [48–51].

The amount of the stratum corneum that is removed by peeling of an adhesive tape depends on many factors, including the strength of the adhesive. Pinkus [52] used Scotch® tape and reported that two-thirds of the tape was covered with a layer of cells after the first strip, and between one-half and two-thirds was covered after each subsequent strip with new tape. Bommannan *et al.* [53] concluded that one layer of corneocytes was removed with each strip during their tests. Depending on the tape used, between 0 and 90% of the tape was covered by stratum corneum cells in tests by Dykes *et al.* [11], while ranges of 4–66% and 13–87% were obtained in [54] and [55], respectively.

Bothwell [56] applied tape segments with width-to-length dimensions of 25.4×50.8 mm to the backs of six subjects. Peel forces were

typically in the range of 1–3 N. Large amounts of stratum corneum cells usually adhered to occlusive tapes, and small amounts to permeable (nonocclusive) tapes. Up to 40 strips were used, and the peel force tended to increase for the first 15–20 strips. Andrews *et al.* [57] applied a 10×140 mm tape to the subject's volar forearm, which was held at a fixed angle and faced downward. A weight was attached to the hanging end of the tape, and the peel rate was determined. The authors obtained a mean interfacial energy of $14\,J/m^2$, half of what they found when the substrate was glass.

Lucast and Taylor [58] applied 25.4 mm wide tapes to the backs of subjects and used a peel angle (*i.e.*, the angle between the detached portion of the tape and the skin from which the tape had been removed) of 180°. The peel force depended on the type of adhesive, and varied from 0.3 to 4.9 N. Spencer *et al.* [59] used 25.4-mm wide strips from adhesive patches, also with a peel angle of 180°. Reported peel forces were in the range of 1.5–1.7 N for dry skin, and 0.3–0.7 N for skin with perspiration. Ko [60] reported peel forces ranging from 0.4 to 3.5 N for a 25.4-mm width of a strip from a transdermal drug delivery patch. Three different pressure-sensitive adhesives were tested. The amount of skin irritation tended to be lower when the peel force was lower and fewer cells were removed from the stratum corneum by the peeling.

Mayrovitz and Carta [61] applied 13×70 mm tapes to the volar forearms of 10 subjects. The mean peel force was 1.2 N (corresponding to 2.3 N if the width were 25.4 mm), which was reduced by about 35% when an adhesive remover product was utilized before peeling. Maillard-Salin *et al.* [62] peeled 10×45 mm samples of patches at 90° from the forearms of 10 subjects. The mean peel force was 1.2 N (*i.e.*, 3.0 N if the width were 25.4 mm). Chivers [6] presented results [also shown in [10]] from peel tests on the forearms of subjects. Most of the measured peel forces for a 25.4-mm width of tape were in the range of 3–8 N.

Gieselman [63] reported results of tests in which 25.4×76 mm samples of Durapore™ surgical tape (with a woven acetate-taffeta backing and a pressure-sensitive acrylic adhesive) were peeled from the backs of subjects. The tape was placed on either side of the spinal column and perpendicular to it, and the peel angle was 180°. For dry skin, the mean peel force was 0.7 N for a dwell time of 5 minutes, and 2.5 N when the dwell time was 48 hours. Other tests using Durapore tape were described by Karwoski [5], Karwoski and Plaut [14], and Plaut and Karwoski [15]. The tape was 25.4-mm wide and was applied for a length of 75 mm along the volar forearm. Peel angles of 90°, 120°, 150°, and 180° were utilized, with peel rates ranging from 100 to

10,000 mm/min. Four subjects participated in the study. Mean peel forces ranged from 0.5 to 2.9 N.

Tokumura *et al.* [54,55,64] used 15-mm wide tapes, a peel angle of 90°, and six, eight, and six subjects, respectively. For the first stripping, the peel forces on a forearm, adjusted to a 25.4-mm width, were 1.8–3.3 N in [64], 0.3–2.5 N in [54], and 0.7–1.3 N in [55]. In [64], as more strips were conducted, the peel force increased and the amount of stripped corneocytes per strip decreased. In [54], tapes were peeled from the forearm, cheek, palm, and sole. For a permeable tape, the mean peel force was lowest for the forearm and highest for the palm, and the standard deviations were high. For an occlusive tape, the variation in peel force with location was much lower.

Four papers by Kiat-amnuay *et al.* [9,65–67] in *The Journal of Prosthetic Dentistry* were related to the behavior of medical adhesives when they retain extraoral maxillofacial prostheses and then are removed from the skin. Peel tests were performed with 20×60 mm strips on the volar forearms of subjects at a 90° angle. In most of the tests, the prosthesis was a 3-mm thick silicone elastomer, which was much stiffer than the backings of the tapes used in the other studies cited here. The tests reported in [9] involved 20 subjects, and the peel force based on a width of 25.4 mm varied from 0.5 to 2.8 N. The other three papers involve variations of those tests, such as multiple strippings, combinations of adhesives, and a chlorinated polyethylene elastomer.

Lir *et al.* [68] described tests involving peeling of tape from the fingers or forearms of 10 subjects at an angle of 180°. The tapes had a width of 25.4 mm and were attached for a length of 80 mm. The mean peel force for a 3-minute dwell time was 5.1 N for Micropore™ tape and 7.4 N for Transpore™, and was about 25 N for a dwell time of 24 hours. The results were compared with those for a substrate of Mylar™ and for a substrate consisting of a thin film developed to mimic the properties of skin. In a similar study, Renvoise *et al.* [8,69] peeled tape from the forearms of four subjects at an angle of 180°. Peel forces up to 13 N for a 25.4-mm width were reported. The peel force tended to increase as further strippings (up to 10) were conducted. These results on *in vivo* skin were compared with data obtained using a synthetic substrate of a biomimetic model material.

2.4. Mathematical Models

In the model considered here, the skin without tape attached to it will only be under tension. For uniaxial, quasi-static tension, skin is initially easy to deform and then becomes quite resistant to further

stretching. The slope of the stress-strain curve tends to increase monotonically, and reported values of Young's modulus, E, for human skin cover four orders of magnitude, from 0.01 to 100 MPa [70]. Mathematical descriptions of the stress-strain relationship of skin in tension have utilized power laws, exponential equations, logarithmic expressions, and strain energy functions [27].

Sometimes skin is modeled as a membrane with a certain effective thickness [71–74]. Bending stiffness is neglected. This type of model will be considered here, but in a two-dimensional cross section (like a cable or string model). It is not appropriate when the skin is compressed along its surface; in that case, wrinkles tend to form and bending resistance should be included. A few references involving compression will be mentioned.

Magnenat-Thalmann *et al.* [75] described two- and three-layer skin models, with each layer being linearly elastic or elastic-plastic. Folds caused by compression were simulated computationally. Flynn and McCormack [76,77] presented one-, two-, and three-layer skin models and used the finite element program ABAQUS. The stress-strain law in compression was hardening. Skin profiles obtained numerically were compared with those from tests on the forearms of eight subjects. Finally, Kuwazuru *et al.* [78] developed a five-layer skin model with a linearly elastic moment-curvature relationship. The skin was modeled as a horizontal, composite, Timoshenko beam comprised of up to four layers. The beam was attached to an underlying elastic foundation consisting of a shear layer and a distribution of vertical springs, and the wavelength of the governing buckling mode was determined.

3. FORMULATION OF MODEL

Figure 1 shows a sketch of a two-dimensional cross section of a piece of adhesive tape attached to a skin surface (originally horizontal) and pulled upward with a high peel angle. The tape consists of a backing

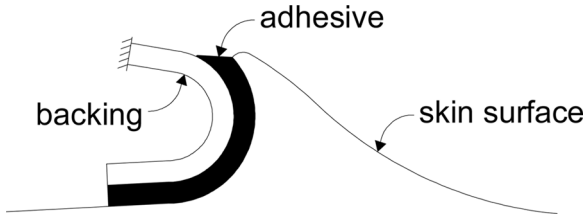

FIGURE 1 Illustration of tape (backing and adhesive) being peeled off skin surface.

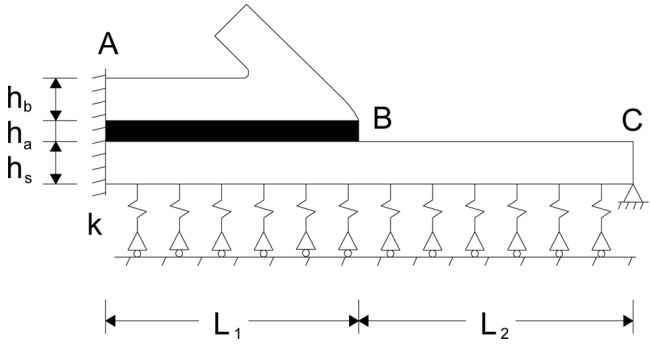

FIGURE 2 Illustration of model before pulling begins.

and an adhesive, and strong adhesion is assumed to occur between the tape and the skin. At the upper end of the detached portion of the tape, the hand applies a displacement, and the attachment is depicted as a fixed end (which, in general, may include a shear force and bending moment as well as a tangential force).

The model to be considered is shown in Fig. 2 before pulling is initiated. The thickness of the backing is h_b, the thickness of the adhesive is h_a, and the skin is modeled as a flexible strip with effective thickness h_s. The width of the tape and skin cross sections is w. Self-weight and prestress in the tape and skin are not included in the analysis. As the skin is pulled upward, there is not much resistance from the subcutaneous tissue, but significant resistance from the skin on both sides, which is represented by a linearly elastic foundation with stiffness k that provides a vertical, distributed, restraining force.

Initially, the horizontal length of the tape attached to the skin surface is L_1 and the remaining length of the skin is L_2. The left end A is assumed to be fixed, and the right end C is assumed to be pinned and immovable. The peel front is denoted B.

A typical deflected shape of the model is presented in Fig. 3 for a peel angle $\theta_p = 170^\circ$. The external force is denoted F and the detached

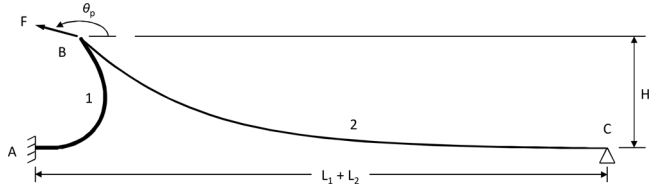

FIGURE 3 Illustration of shape of model with peel angle $\theta_p = 170^\circ$.

tape is assumed to be straight and to contain no shear force or bending moment. The length of the detached tape is not of interest here. A kink is allowed in the tape at B. The kink and the straight shape of the detached tape are approximations of what was observed in the experiments described in [14]. Segment 1 consists of combined tape and skin strips, and Segment 2 only contains the skin strip. The height of the peel front B is denoted H.

Some models related to the present one but not including bending stiffness were considered previously [7,79,80], in which Segments 1 and 2 were straight (along with a straight Segment 3 of the detached tape) and there was no elastic foundation. The peel condition was based on fracture mechanics. In [79], Segments 1 and 2 were inextensible and initially slack, while Segment 3 was extensible. In [7], the tape was inextensible (Segments 1 and 3) and Segment 2 was linearly or nonlinearly elastic. Finally, both the tape and skin were linearly elastic in [80].

Several models that include bending stiffness were investigated in [5]. The tape and skin were each represented as an inextensible elastica, and a horizontal spring was included at the left end, A, and sometimes also at the right end, C, both of which were fixed. Very few numerical results were obtained, and continuity of the slopes of the skin and the tape led to shapes that do not resemble those in Figs. 1 and 3. The analytical and numerical work in [5] comprised preliminary research for the present paper.

In Segment 1, with the tape and skin attached, it is assumed here that the tape backing dominates the behavior. The segment is modeled as a linearly elastic, extensible elastica with modulus of elasticity E_1, effective area $A_1 = h_b w$, and effective moment of inertia $I_1 = h_b^3 w/12$. The skin in Segment 2 is modeled as an extensible strip having no bending resistance, and, therefore, no bending moment or shear force. The effective area is $A_2 = h_s w$. The stress-strain relationship in Segment 2 is chosen to have a form similar to that in the experimental results reported in [31] and is plotted in Fig. 4. In the cases examined here, only tension occurs in Segment 2; however, compression occurs in the lower portion of Segment 1 for peel angles larger than about 100°, and, therefore, bending stiffness is included in that segment.

Free body diagrams of portions of Segments 1 and 2 adjacent to the ends are depicted in Figs. 5a and 5b, respectively. In Segment 1, the undeformed arc length is s_1, the horizontal coordinate is $x_1(s_1)$, the vertical coordinate is $y_1(s_1)$, the rotation is $\theta_1(s_1)$, the bending moment is $M_1(s_1)$, the constant internal horizontal force is P_1, and the internal vertical force is $Q_1(s_1)$. In Segment 2, the undeformed arc length is s_2, the horizontal coordinate is $x_2(s_2)$, the vertical coordinate is

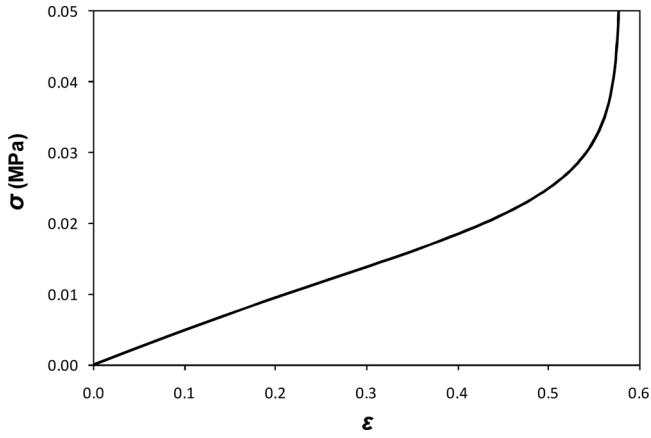

FIGURE 4 Assumed stress-strain relationship of skin.

$y_2(s_2)$, the rotation is $\theta_2(s_2)$, and the tensile force is $T_2(s_2)$. Positive senses are as shown. A second subscript indicates the location, *i.e.*, point A, B, or C.

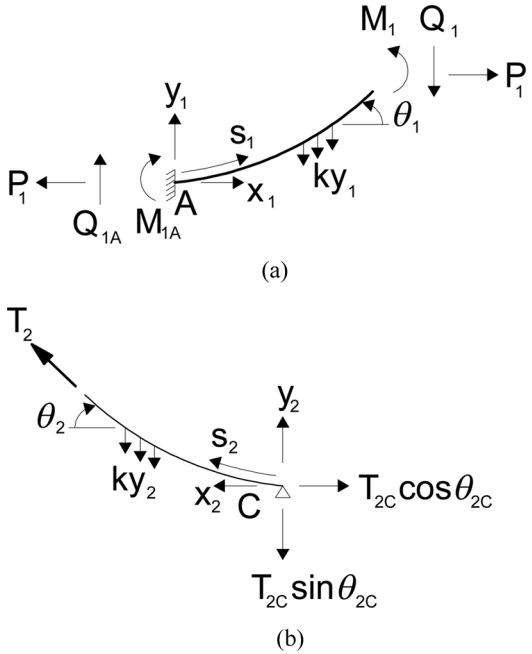

FIGURE 5 Free body diagrams of model at (a) left end and (b) right end.

Based on geometry, equilibrium, and the constitutive law, the governing equations in Segment 1 are [81]

$$\frac{dx_1}{ds_1} = (1+\varepsilon_1)\cos\theta_1, \quad \frac{dy_1}{ds_1} = (1+\varepsilon_1)\sin\theta_1, \quad \frac{d\theta_1}{ds_1} = \frac{M_1}{E_1 I_1},$$

$$\frac{dM_1}{ds_1} = (1+\varepsilon_1)\,(Q_1\cos\theta_1 + P_1\sin\theta_1), \quad \frac{dQ_1}{ds_1} = -ky_1, \tag{1}$$

where

$$\varepsilon_1 = \frac{P_1\cos\theta_1 - Q_1\sin\theta_1}{E_1 A_1}. \tag{2}$$

The governing equations in Segment 2 are

$$\frac{dx_2}{ds_2} = (1+\varepsilon_2)\cos\theta_2, \quad \frac{dy_2}{ds_2} = (1+\varepsilon_2)\sin\theta_2,$$
$$\frac{d\theta_2}{ds_2} = \frac{ky_2\cos\theta_2}{T_2}, \quad \frac{dT_2}{ds_2} = ky_2\sin\theta_2, \tag{3}$$

with the strain assumed to be given by

$$\varepsilon_2 = 20\sigma_2\left[\frac{1+(40\sigma_2)^2}{1+(40\sigma_2)^4}\right]^{0.45}, \quad \text{where } \sigma_2 = \frac{T_2}{A_2}. \tag{4}$$

The unit of stress in Eq. (4) is MPa. (The form of Eq. (4) was used in [82] for a moment-curvature relationship.)

The boundary conditions at $s_1 = 0$ (the left end, point A) are $x_1 = 0$, $y_1 = 0$, and $\theta_1 = 0$. Since the bending moment in Segment 1 should be small, $M_1(0)$ is also set equal to zero. At $s_2 = 0$ (the right end, point C), the conditions are $x_2 = 0$ and $y_2 = 0$. Also, it is desired to set $\theta_2 = 0$ at C, but this causes numerical difficulties, so $\theta_2(0) = 0.01 = 0.57^\circ$ is used in the solution procedure. (If this value is doubled or halved, the results are not altered significantly.) It is noted that the values of M_1 at A and θ_2 at C are not natural boundary conditions, but can be specified here since the lengths L_1 and L_2 will be treated as unknown variables.

At point B, where $s_1 = L_1$ and $s_2 = L_2$, the conditions are

$$x_{1B} + x_{2B} = L_1 + L_2, \;\; y_{1B} = H, \;\; y_{2B} = H, \;\; M_{1B} = 0, \;\; T_{2B}\sin(\theta_{2B} + \theta_p) = P_1\sin\theta_p + Q_{1B}\cos\theta_p. \tag{5}$$

The last two of these conditions are based on equilibrium at B, which also yields the following formula that provides the value of

the external force, F, from the numerical results:

$$F = \frac{(T_{2B}\sin\theta_{2B} - Q_{1B})}{\sin\theta_p}. \tag{6}$$

Numerical solutions are obtained using a shooting method with the subroutines NDSolve and FindRoot in Mathematica [83]. The quantities L_1, L_2, P_1, $Q_1(0)$, and $T_2(0)$ are varied until Eqs. (5) are satisfied with sufficient accuracy (*e.g.*, five significant digits). Therefore, in this analysis, the lengths L_1 and L_2 are not specified, but are obtained as part of the solution. In the cases considered here, as the tape is pulled, L_2 increases for $\theta_p = 90^\circ$, 120°, 150°, and 170°, whereas L_1 increases if $\theta_p = 90^\circ$, but initially decreases and then increases for the other three peel angles. (In Section 4.5, the analysis will be modified and L_2 will be specified.)

4. RESULTS

4.1. Parameters

In the numerical work, lengths are given in mm and forces in N, so that stresses are in N/mm^2, *i.e.*, in MPa. The tape parameters are chosen to be $w = 25.4$ mm, $h_b = 0.15$ mm, and $E_1 = 800$ MPa (which gives $E_1A_1 = 3{,}050$ N and $E_1I_1 = 5.72$ N-mm^2). These quantities correspond to test results for Durapore surgical tape [5], in which the tensile stress-strain relationship is almost linear for the range of stresses involved here. (The strain in Segment 1 of the model ranges from -0.0002 to 0.0006 in the numerical results to be presented.)

For the skin, the effective thickness is assumed to be $h_s = 1$ mm, and the total downward vertical component of the resisting stiffness from the skin on the sides of the 25.4-mm width in the model is chosen to be $k = 0.01$ MPa (except in Section 4.4 where the effect of changes in k is examined). This value of k leads to forces and displacements similar to those found in the peel tests reported in [5,14,15]. Based on Eq. (4), which is plotted as stress *versus* strain in Fig. 4, the initial ratio of stress to strain for the skin is 0.05 MPa, and the "knee" of the curve occurs in a region around $\varepsilon = 0.5$ and $\sigma = 0.025$ MPa. The maximum strain in Segment 2 of the model occurs at B (see Fig. 3), and with this constitutive law, peeling would be expected to occur sometime after ε_{2B} reaches 0.5. A bilinear approximation for Eq. (4) is $\varepsilon = 20\sigma$ for $0 \le \sigma \le 0.025$, and $\varepsilon = 2\sigma + 0.45$ for $\sigma > 0.025$, but this is not used here.

The behavior during pulling of the tape will be described in the next section. Peeling will be discussed in Section 4.3. As an example of the parameters obtained, the shape in Fig. 3 corresponds to the case $\theta_p = 170^\circ$ and $H = 6.95$ mm, for which $\theta_{1B} = 126^\circ$, $\theta_{2B} = 48^\circ$, $L_1 = 10.7$ mm, $L_2 = 28.5$ mm, $P_1 = -0.29$ N, $Q_{1A} = 0.56$ N, $T_{2C} = 0.36$ N, $T_{2B} = 0.53$ N, and $\varepsilon_{2B} = 0.45$.

4.2. Pulling with Four Different Peel Angles

Figure 6 shows shapes for peel angle $\theta_p = 90^\circ$ when the height of the peak (point B) is $H = 2$, 6, 10, and 14 mm, respectively. (In this case, $P_1 = T_{2C}\cos\theta_{2C}$ due to overall horizontal equilibrium.) The corresponding external forces F are 0.13, 0.60, 1.30, and 2.24 N, respectively.

Plots of F *versus* H are presented in Fig. 7 for $\theta_p = 90^\circ$, 120°, 150°, and 170°. The points (H, F) for the four cases in Fig. 6 are included in the curve for $\theta_p = 90^\circ$. The curves tend to be convex for $\theta_p = 90^\circ$ and 120°, and concave for $\theta_p = 150^\circ$ and 170°.

The curves for $\theta_p = 150^\circ$ and 170° end when Segments 1 and 2 become parallel at the peak B, with $H = 7.9$ mm, $\theta_{1B} = 130.8^\circ$, and $\theta_{2B} = 49.2^\circ$ if $\theta_p = 150^\circ$, and $H = 7.0$ mm, $\theta_{1B} = 133.5^\circ$, and $\theta_{2B} = 46.5^\circ$ if $\theta_p = 170^\circ$. For larger values of H, the model does not yield physically meaningful solutions (*i.e.*, there is penetration of Segment 1 into Segment 2 near B). The curve for $\theta_p = 170^\circ$ has a negative slope near where it ends, but this does not imply instability since displacement control is considered rather than force control (*i.e.*, H is increased).

The maximum axial strain in Segment 2 occurs at the peak B and is plotted as a function of H in Fig. 8. For a given value of H, ε_{2B} increases as θ_p increases. For $\theta_p = 90^\circ$, 120°, and 150°, respectively, ε_{2B} reaches 0.5 at (H, F) = (10.1 mm, 1.32 N), (9.3 mm, 0.96 N), and (7.9 mm, 0.75 N).

Figure 9 shows the maximum tension, T_{2B}, in Segment 2 as a function of H. The maximum tension increases as the tape is pulled upward, as does the rate of increase of T_{2B}. For a given value of H, T_{2B} increases as the peel angle increases.

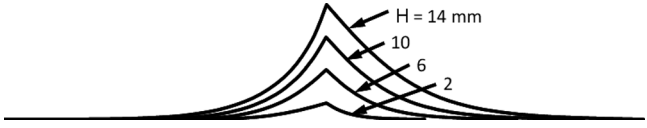

FIGURE 6 Shapes of model for $\theta_p = 90^\circ$ and $H = 2$, 6, 10, and 14 mm.

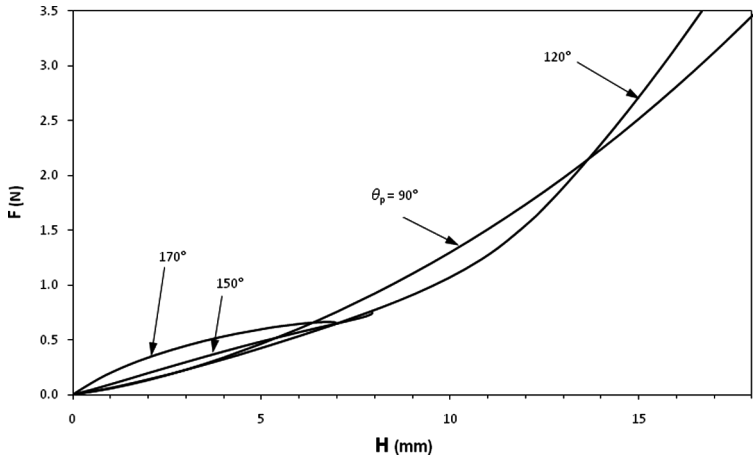

FIGURE 7 External force F *versus* height H for $\theta_p = 90°$, 120°, 150°, and 170°.

4.3. Peel Force

Various criteria have been proposed to predict the value of an increasing external force at which peeling begins. Sometimes the adhesive in the neighborhood is modeled as stretching fibrils [84,85], and a critical value of the force (or extension) in the fibril at the peel front is assumed to govern debonding [85,86]. A simple criterion related to the parameters in the present model will be considered.

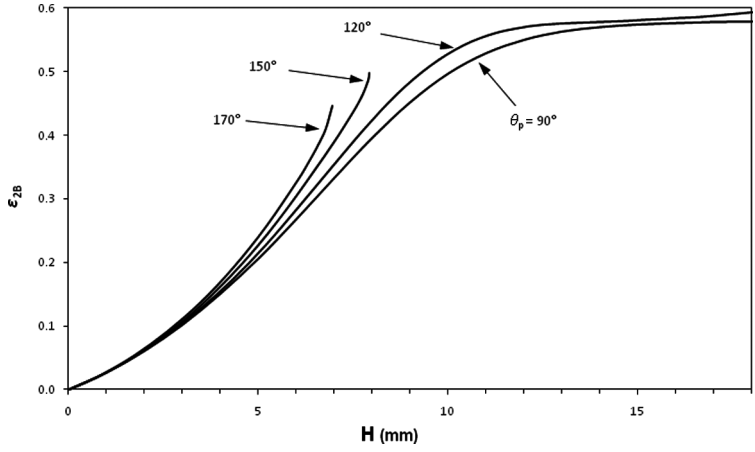

FIGURE 8 Maximum skin strain ε_{2B} *versus* height H for $\theta_p = 90°$, 120°, 150°, and 170°.

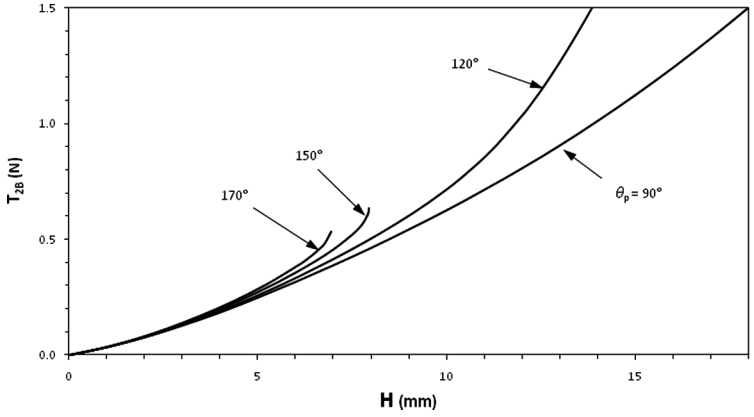

FIGURE 9 Maximum skin tension T_{2B} *versus* height H for $\theta_p = 90°$, 120°, 150°, and 170°.

The direction of Segment 2 at the peak B (see Figs. 1 and 3) is approximately the same as the direction of this last fibril. From equilibrium at B, the tension, T_{2B}, in Segment 2 is expected to be close to the force in the last fibril. A possible criterion for peeling to be initiated is that T_{2B} reaches a critical value. The corresponding external force, F, will be called the peel force, F_p. For critical values $T_{2B} = 0.5, 0.6, \ldots,$ 1.0 N, Fig. 10 shows how F_p depends on the peel angle θ_p. Except for

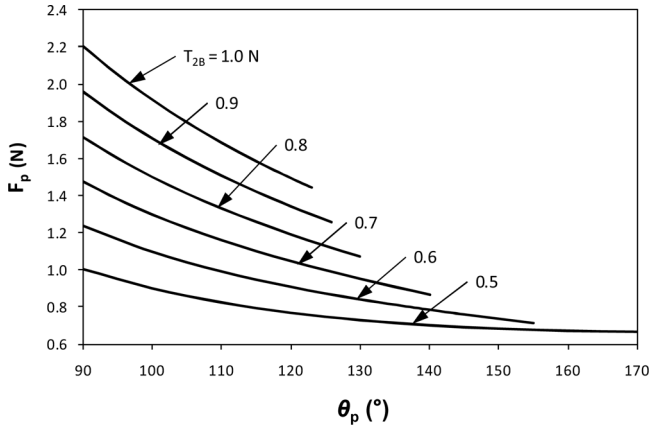

FIGURE 10 Peel force F_p *versus* peel angle θ_p for peel criterion $T_{2B} = 0.5$, 0.6, 0.7, 0.8, 0.9, and 1.0 N.

$T_{2B} = 0.5$ N in the figure, the curves end when Segments 1 and 2 become parallel at B and the model becomes inapplicable. The corresponding strains ε_{2B} on the curves for $T_{2B} = 0.5, 0.6, \ldots,$ 1.0 N, respectively, are 0.42, 0.48, 0.52, 0.55, 0.56, and 0.57, independent of θ_p.

In Fig. 10, the peel force decreases as the peel angle increases (till each curve ends). This is the typical behavior for peeling of a pressure-sensitive tape from a rigid surface, at least for the initial parts of the curve starting at $\theta_p = 90^\circ$ [6,80,87–90]. For the six sets of experimental results on skin with variable peel angle in [5,14], using $\theta_p = 90^\circ$, 120°, 150°, and 180°, the plot of peel force *versus* peel angle exhibited a minimum at 120° for one test, a minimum at 150° for four tests, and a monotonic decrease from 90° to 180° in the other case.

4.4. Effect of Side Stiffness

In the two-dimensional model used here, the resistance to uplift of the skin strip is caused by the tension in the strip and by the skin on the sides of the strip (plus a possible small contribution from the underlying material). The stiffness, k, of the elastic foundation representing the resistance from outside the strip was chosen to be 0.01 MPa in the standard case. The effect of doubling or halving this value is examined in Figs. 11–13 for peel angle $\theta_p = 120^\circ$.

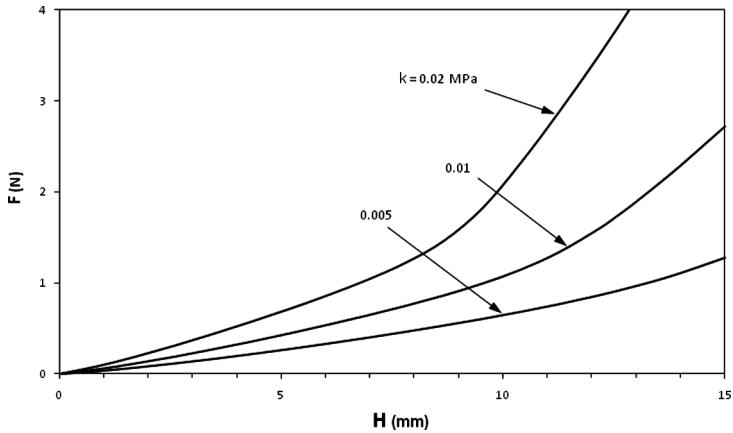

FIGURE 11 External force F *versus* height H for $\theta_p = 120^\circ$ and $k = 0.005$, 0.01, and 0.02 MPa.

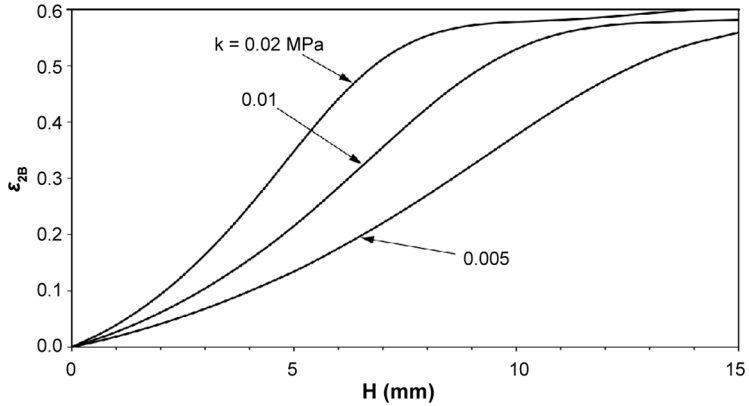

FIGURE 12 Maximum skin strain ε_{2B} *versus* height H for $\theta_p = 120^\circ$ and $k = 0.005$, 0.01, and 0.02 MPa.

The middle curves, for $k = 0.01$, are the same as in Figs. 7–9, respectively, but in Figs. 11–13 the limit on the height H is 15 mm instead of 18 mm. For a given value of H in Figs. 11–13, the external force, maximum strain, ε_{2B}, in Segment 2, and maximum tension, T_{2B}, in Segment 2 increase as k increases. If the external force F were fixed, the quantities H, ε_{2B}, and T_{2B} all would decrease as k increases.

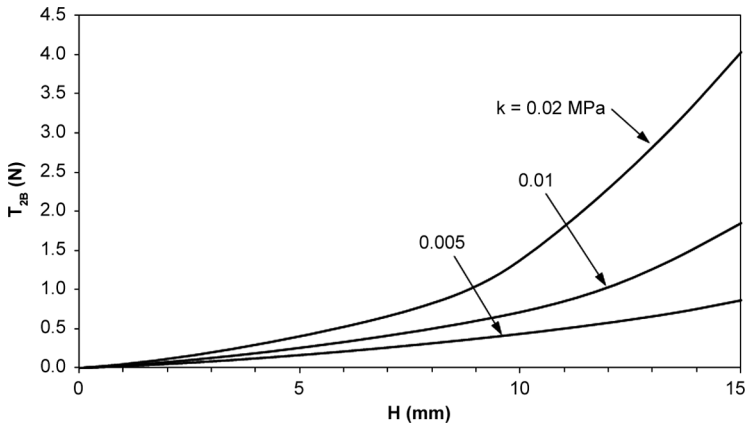

FIGURE 13 Maximum skin tension T_{2B} *versus* height H for $\theta_p = 120^\circ$ and $k = 0.005$, 0.01, and 0.02 MPa.

4.5. Holding Skin Down

When peeling adhesive tape from skin, sometimes the skin ahead of the peel front is held down [6]. To model this situation, the undeformed length L_2 of Segment 2 is fixed at 5 or 10 mm (see Figs. 2 and 3). To replace the variable L_2 in the analysis, the rotation at the right end C is allowed to vary, instead of being fixed at $\theta_2(0) = 0.01$. This results in the shape of Segment 2 being almost linear from B to C.

Results were obtained for the case $\theta_p = 90^\circ$ and are presented in Figs. 14–16. The curves marked "unrestricted" correspond to the previous analysis in which L_2 was one of the variables and $\theta_2(0) = 0.01$. In Fig. 14, the external force, F, is plotted *versus* the height, H. For a given value of H, the force, F, increases as the length of Segment 2 decreases (*i.e.*, as the constraint location moves closer to the peel front).

The maximum tension, T_{2B}, in Segment 2 is plotted *versus* H in Fig. 15. The behavior is similar to that in Fig. 14. Finally, in Fig. 16, T_{2B} is plotted as a function of F. For a given value of F, T_{2B} increases as the length of Segment 2 decreases. Therefore, based on the results in Fig. 16, if debonding begins when T_{2B} reaches a critical value, the peel force would decrease as the skin is held down closer to the peel front (*i.e.*, as L_2 is decreased).

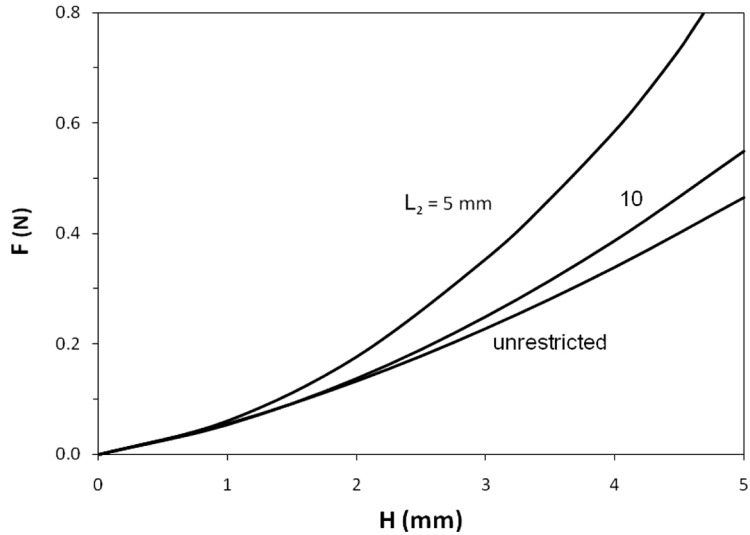

FIGURE 14 External force F *versus* height H for $\theta_p = 90^\circ$ and $L_2 = 5$ mm, 10 mm, and unrestricted.

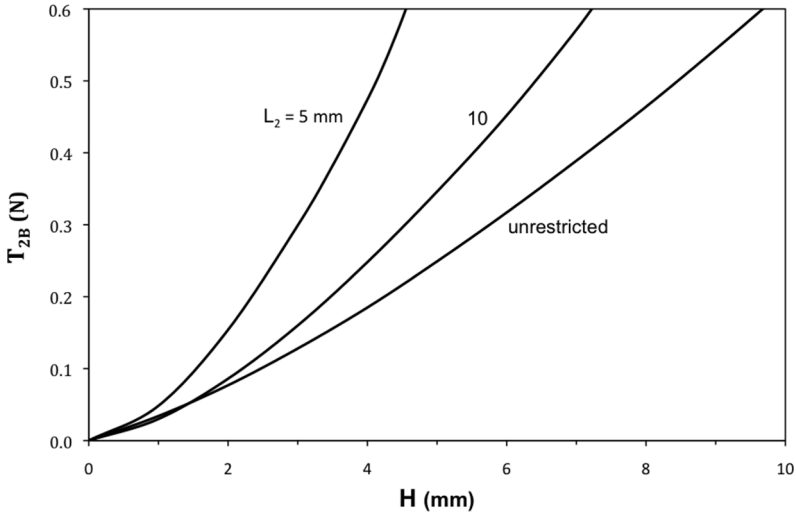

FIGURE 15 Maximum skin tension T_{2B} *versus* height H for $\theta_p = 90^\circ$ and $L_2 = 5$ mm, 10 mm, and unrestricted.

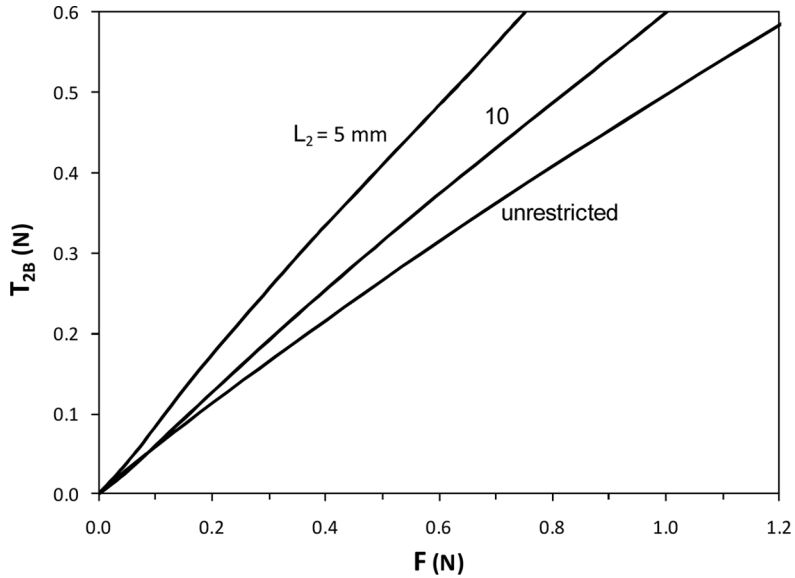

FIGURE 16 Maximum skin tension T_{2B} *versus* external force F for $\theta_p = 90^\circ$ and $L_2 = 5$ mm, 10 mm, and unrestricted.

5. CONCLUDING REMARKS

The literature on peeling of adhesive tape from human skin was reviewed. Then a simple two-dimensional analytical model was formulated, and numerical results were obtained. Modeling the peeling of tape with strong adhesion from human skin is difficult. Large rotations and large strains in the skin are involved, and the constitutive behavior of skin is highly nonlinear. Many assumptions were made in the model. The magnitudes of the resulting forces and displacements were similar to those obtained in experiments described in [5,14,15].

Various extensions of the model are possible. Prestress in the skin and/or tape could be included [77]. According to [91], which describes damage to skin due to taping, nurses often apply tape under tension to cause compression in the skin following surgical or diagnostic procedures.

The self-weight of the tape and/or skin also could be added to the model. The bending stiffness of the skin could be considered, and it would be helpful if experimental data for the moment-curvature relationship (for both concave and convex displacements) would become available. Also, test data on the constitutive behavior for compression along the skin surface would be useful.

Shear resistance of the side skin could be included, *e.g.*, by fixing the lower end of the foundation so that the distributed springs do not remain vertical, or by adding a shear layer under the skin strip [78]. The constitutive law for the foundation could be nonlinear, resembling that for the skin in tension. The substrate could be initially curved [85,92]. Also, fibrils could be modeled, such as in a zone near the peel front [85], with the skin strip possibly exhibiting its maximum possible concave curvature within or near that zone (see Fig. 1). The behavior near the peel front may have some similarity to that in an asymmetric T-peel test [93,94].

Since the substrate deforms during pulling, the puller may tend to vary the peel angle (*e.g.*, to try to keep one of the local, relative angles between the detached tape and the skin surface constant [79,80]). This could be incorporated in the numerical procedure.

In tests with high peel angles, waves often occurred in the tape attached to the skin [5], but the present model did not produce such waves. The wavelength is much longer than that for wrinkling of skin under compression along the surface. Perhaps a generalization of the model could yield such waves, although they may not have much effect on the peeling process. The behavior of the foundation should be different for indentation (due to waves) than for outward deformation.

Plasticity in the backing could be modeled, as well as rate effects. Skin exhibits viscoelastic behavior [4,95], as do pressure-sensitive adhesives. An approach similar to that used in [96] for a linear viscoelastic adhesive might be applicable to determine the effect of the peel rate on the peel force.

Since the skin surface can slide along the subcutaneous fat, it seemed logical to model the skin as a flexible strip. However, it could also be modeled as a deformable continuum [97–99].

The peel criterion could be based on fracture mechanics [93,100]. Then the experimental data on the cohesive strength of the outer cell layers in the stratum corneum (see Section 2.2) could be incorporated in the analysis.

Three-dimensional analyses, perhaps using the finite element method, should be conducted. They could capture the ridges emanating to the sides of the peel front, and the curvature of the peel front across the width of the tape (see Fig. 2.15 of [5], and [101]).

When a pressure-sensitive tape is peeled from a rigid substrate, sometimes stick-slip behavior is observed (*e.g.*, [102,103]). Friction tests with a rigid spherical probe moving on skin have exhibited stick-slip [38,39]. Therefore, it is expected that stick-slip will occur when peeling pressure-sensitive tape from skin under some circumstances, and a dynamic analysis might uncover such a phenomenon.

In conclusion, pulling and peeling of a tape with a strong adhesive from a highly deformable surface at high peel angles is much more complicated to analyze than peeling from a rigid substrate. Human skin is a highly variable material with solid and fluid components. Peeling may be governed by failure between cell layers at and underneath the skin surface, rather than failure between the adhesive and the skin, or within the adhesive. Much work remains to be done on this important and challenging problem.

ACKNOWLEDGMENTS

The author is grateful for assistance on this and related research from Alicia C. Karwoski, David A. Dillard, Eugene G. Joseph, Daniel Post, Benjamin Z. Dymond, Rachel V. Kozink, Stacy L. Coulthard, Robert Simonds, Don C. Ohanehi, and the Optical Sciences and Engineering Research Center at Virginia Tech. The author is also grateful to the reviewers for their helpful suggestions.

REFERENCES

[1] Satas, D., Medical products, in *Handbook of Pressure Sensitive Adhesive Technology*, 3rd ed., D. Satas (Ed.) (Satas and Associates, Warwick, Rhode Island, 1999), pp. 706–723.

[2] Lucast, D. H., *Adhesives Age* **43**, 36–39 (2000).

[3] Gniadecka, M. and Serup, J., Medical products, in *Handbook of Non-Invasive Methods and the Skin*, J. Serup and G. B. E. Jemec (Eds.) (CRC Press, Boca Raton, Florida, 1995), pp. 329–334.

[4] Barel, A. O., Lambrecht, R., and Clarys, P., *Curr. Probl. Dermatol.* **26**, 69–83 (1998).

[5] Karwoski, A. C., *"Testing and analysis of the peeling of medical adhesives from human skin,"* (M.S. Thesis, Virginia Polytechnic Institute and State University, Blacksburg, VA, USA, 2003). Online: http://scholar.lib.vt.edu/theses/available/etd-05292003-114935.

[6] Chivers, R. A., *Int. J. Adhesion Adhesives* **21**, 381–388 (2001).

[7] Steven-Fountain, A. J., Atkins, A. G., Jeronimidis, G., Vincent, J. F. V., Farrar, D. F., and Chivers, R. A., *Int. J. Adhesion Adhesives* **22**, 423–430 (2002).

[8] Renvoise, J., Burlot, D., Marin, G., and Derail, C., *Int. J. Pharm.* **368**, 83–88 (2009).

[9] Kiat-amnuay, S., Gettleman, L., and Goldsmith, L. J., *J. Prosthet. Dent.* **84**, 335–340 (2000).

[10] Webster, I., *Int. J. Adhesion Adhesives* **19**, 29–34 (1999).

[11] Dykes, P. J., Heggie, R., and Hill, S. A., *J. Wound Care* **10**, 7–10 (2001).

[12] Dykes, P. J. and Heggie, R., *J. Wound Care* **12**, 260–262 (2003).

[13] Murahata, R. I., Taylor, M. G., Damia, J., and Grove, G. L., *Skin Research Technol.* **14**, 1–6 (2008).

[14] Karwoski, A. C. and Plaut, R. H., *Skin Research Technol.* **10**, 271–277 (2004).

[15] Plaut, R. H. and Karwoski, A. C., Tests on peeling of adhesive tape from human skin, *Proceedings of the 18th ASCE Engineering Mechanics Division Conference*, M. R. Hajj (Ed.) (Blacksburg, Virginia, 2007).

[16] Furyk, J. S., O'Kane, C. J., Aitken, P. J., Banks, C. J., and Kault, D. A., *Med. J. Australia* **191**, 682–683 (2009).

[17] Koutroupi, K. S. and Barbenel, J. C., *J. Biomech.* **23**, 281–287 (1990).

[18] Marks, R., Lévêque, J.-L., and Voegeli, R., (Eds.) *The Essential Stratum Corneum*, (Martin Dunitz, London, 2002).

[19] Silver, F. H., Siperko, L. M., and Seehra, G. P., *Skin Research Technol.* **9**, 3–23 (2003).

[20] Subramanyan, K., Misra, M., Mukherjee, S., and Ananthapadmanabhan, K. P., *MRS Bull.* **32**, 770–778 (2007).

[21] Farage, M. A., Miller, K. W., and Maibach, H. I., Degenerative changes in aging skin, in *Textbook of Aging Skin*, M. A. Farage, K. W. Miller, and H. I. Maibach (Eds.) (Springer, Berlin, 2010), pp. 25–35.

[22] Carrougher, G. J., *Burn Care and Therapy*, (Mosby, St. Louis, Missouri, 1998).

[23] Piérard, G. E., *Skin Pharm. Appl. Skin Physiol.* **12**, 352–362 (1999).

[24] Sanders, J. E., Goldstein, B. S., and Lotta, D. F., *J. Rehab. Res. Devel.* **32**, 214–226 (1995).

[25] Yannis, I. V., in *The Biomedical Engineering Handbook*, J. D. Bronzino (Ed.) (CRC Press, Boca Raton, Florida, 1995), pp. 2025–2038.

[26] Fung, Y. C., *Biomechanics: Mechanical Properties of Living Tissues*, 2nd ed., (Springer-Verlag, New York, 1993).

[27] Lanir, Y., Skin mechanics, in *Handbook of Bioengineering*, R. Skalak and S. Chien (Eds.) (McGraw-Hill, New York, 1987), pp. 11.1–11.25.
[28] Borges, A. F., *Plastic Reconstructive Surgery* **73**, 144–150 (1984).
[29] Piérard, G. E., Nikkels-Tassoudji, N., and Piérard-Franchimont, C., *Dermatol.* **191**, 9–15 (1995).
[30] Diridollou, S., Berson, M., Vabre, V., Black, D., Karlsson, B., Auriol, F., Gregoire, J. M., Yvon, C., Vaillant, L., Gall, Y., and Patat, F., *Ultrasound Med. Biol.* **24**, 215–224 (1998).
[31] Kvistedal, Y. A. and Nielsen, P. M. F., *Biomech. Model. Mechanobiol.* **8**, 1–8 (2009).
[32] Serup, J., Jemec, B. E., and Grove, G. L. (Eds.) *Handbook of Non-Invasive Methods and the Skin*, 2nd ed., (Taylor & Francis, Boca Raton, Florida, 2006).
[33] Delalleau, A., Josse, G., Lagarde, J.-M., Zahouani, H., and Bergheau, J.-M., *Inverse Prob. Sci. Eng.* **16**, 325–347 (2008).
[34] Delalleau, A., Josse, G., Lagarde, J.-M., Zahouani, H., and Bergheau, J.-M., *J. Biomech.* **39**, 1603–1610 (2005).
[35] Dikstein, S. and Fluhr, J. W., Indentometry, in *Handbook of Non-Invasive Methods and the Skin*, 2nd ed., J. Serup, G. B. E. Jemec, and G. L. Grove (Eds.) (Taylor & Francis, Boca Raton, Florida, 2006), pp. 617–620.
[36] Jachowicz, J., McMullen, R., and Prettypaul, D., *Skin Research Technol.* **14**, 312–319 (2008).
[37] Kwiatkowska, M., Franklin, S. E., Hendriks, C. P., and Kwiatkowski, K., *Wear* **267**, 1264–1273 (2009).
[38] Zahouani, H., Pailler-Mattei, C., Sohm, B., Vargiolu, R., Cenizo, V., and Debret, R., *Skin Research Technol.* **15**, 68–76 (2009).
[39] Pailler-Mattei, C., Pavan, S., Vargiolu, R., Pirot, F., Falson, F., and Zahouani, H., *Wear* **263**, 1038–1043 (2007).
[40] Horstmann, M., Müller, W., and Asmussen, B., Principles of skin adhesion and methods for measuring adhesion of transdermal systems, in *Bioadhesive Drug Delivery Systems: Fundamentals, Novel Approaches, and Development*, E. Mathiowitz, D. E. Chickering, and C.-M. Lehr (Eds.) (Marcel Dekker, New York, 1999), pp. 175–195.
[41] Edwards, C., Methods to determine desquamation rate, in *Handbook of Non-Invasive Methods and the Skin*, 2nd ed., J. Serup, G. B. E. Jemec, and G. L. Grove (Eds.) (Taylor & Francis, Boca Raton, Florida, 2006), pp. 361–369.
[42] Alikhan, A. and Maibach, H. I., Biology of stratum corneum: Tape strippling and protein quantification, in *Textbook of Aging Skin*, M. A. Farage, K. W. Miller, and H. I. Maibach (Eds.) (Springer, Berlin, 2010), pp. 401–407.
[43] Marks, R., Nicholls, S., and Fitzgeorge, D., *J. Invest. Dermatol.* **69**, 299–302 (1977).
[44] Marks, R., Quantification of desquamation and stratum corneum cohesivity, in *Cutaneous Investigation in Health and Disease*, J.-L. Lévêque (Ed.) (Marcel Dekker, New York, 1989), pp. 33–47.
[45] Wu, K. S., van Osdol, W. W., and Dauskardt, R. H., *Biomater.* **27**, 785–795 (2006).
[46] Wu, K. S., Li, J., Ananthapadmanabhan, K. P., and Dauskardt, R. H., *J. Mater. Sci.* **42**, 8986–8994 (2007).
[47] Levi, K., Baxter, J., Meldrum, H., Misra, M., Pashkovski, E., and Dauskardt, R. H., *J. Invest. Dermatol.* **128**, 2345–2347 (2008).
[48] Löffler, H., Dreher, F. D., and Maibach, H. I., *Br. J. Dermatol.* **151**, 746–752 (2004).
[49] Escobar-Chávez, J. J., Merino-Sanjuán, V., López-Cervantes, M., Urban-Morlan, Z., Piñón-Segundo, E., Quintanar-Guerrero, D., and Ganen-Quintanar, A., *J. Pharm. Pharmaceut. Sci.* **11**, 104–130 (2008).

[50] Lademann, J., Jacobi, U., Surber, C., Weigmann, H.-J., and Fluhr, J. W., *Eur. J. Pharm. Biopharm.* **72**, 317–323 (2009).
[51] Padula, C., Fulgoni, A., and Santi, P., *Skin Research Technol.* **16**, 125–130 (2010).
[52] Pinkus, H., *J. Invest. Dermatol.* **16**, 383–386 (1951).
[53] Bommannan, D., Potts, R. O., and Guy, R. H., *J. Invest. Dermatol.* **95**, 403–408 (1990).
[54] Tokumura, F., Yoshiura, Y., Homma, T., and Nukatsuka, H., *Skin Research Technol.* **12**, 178–182 (2006).
[55] Tokumura, F., Homma, T., Tomiya, T., Kobayashi, Y., and Matsuda, T., *Skin Research Technol.* **13**, 211–216 (2007).
[56] Bothwell, J. W., Effects of surgical tapes on skin, in *Adhesion in Biological Systems*, R. S. Manly (Ed.) (Academic Press, New York, 1970), pp. 215–221.
[57] Andrews, E. H., Khan, T. A., and Lockington, N. A., *J. Mater. Sci.* **22**, 2833–2841 (1987).
[58] Lucast, D. H. and Taylor, C. W., *Tappi J.* **73**, 159–163 (1990).
[59] Spencer, T. S., Smith, S. E., and Conjeevaram, S., Adhesive interactions between polymers and skin in transdermal delivery systems, in *Polymeric Materials: Science and Engineering*, (American Chemical Society, Washington, DC, 1990), Vol. 63, pp. 337–339.
[60] Ko, C. U., Effect of skin penetration enhancers in transdermal drug delivery adhesives on skin adhesion and irritation, in *Proceedings of the 23rd International Symposium on Controlled Release of Bioactive Materials*, Controlled Release Society, Lincolnshire, Illinois (1996), pp. 281–282.
[61] Mayrovitz, H. N. and Carta, S. G., *Adv. Wound Care* **9**, 38–42 (1996).
[62] Maillard-Salin, D. G., Bécourt, P., and Couarraze, G., *Int. J. Pharm.* **199**, 29–38 (2000).
[63] Gieselman, M. B., U.S. Patent No. US 6,441,092 B1, 2002. Online: http://www.freepatentsonline.com/6441092.html
[64] Tokumura, F., Umekage, K., Sado, M., Otsuka, S., Suda, S., Taniguchi, M., Yamori, A., Nakamura, A., Kawai, J., and Oka, K., *Skin Research Technol.* **11**, 102–106 (2005).
[65] Kiat-amnuay, S., Gettleman, L., and Goldsmith, L. J., *J. Prosthet. Dent.* **85**, 438–441 (2001).
[66] Kiat-amnuay, S., Gettleman, L., and Goldsmith, L. J., *J. Prosthet. Dent.* **92**, 294–298 (2004).
[67] Kiat-amnuay, S., Waters, P. J., Roberts, D., and Gettleman, L., *J. Prosthet. Dent.* **99**, 483–488 (2008).
[68] Lir, I., Haber, M., and Dodiuk-Kenig, H., *J. Adhesion Sci. Technol.* **21**, 1497–1512 (2007).
[69] Renvoise, J., Burlot, D., Marin, G., and Derail, C., Adhesion of PSAS on human skin: A better understanding of the mechanisms, *Proceedings of the 30th Annual Meeting of the Adhesion Society*, (Tampa, Florida, 2007), pp. 273–275.
[70] Rodrigues, L., *Skin Pharm. Appl. Skin Physiol.* **14**, 52–67 (2001).
[71] Danielson, D. A., *J. Biomech.* **6**, 539–546 (1973).
[72] Diridollou, S., Patat, F., Gens, F., Vaillant, L., Black, D., Lagarde, J. M., Gall, Y., and Berson, M., *Skin Research Technol.* **6**, 214–221 (2000).
[73] Cavicchi, A., Gambarotta, L., and Massabò, R., *Finite Elem. Anal. Des.* **45**, 519–529 (2009).
[74] Evans, S. L., *Comput. Meth. Biomech. Biomed. Eng.* **12**, 319–332 (2009).
[75] Magnenat-Thalmann, N., Kalra, P., Lévêque, J. L., Bazin, R., Batisse, D., and Querleux, B., *IEEE Trans. Inf. Technol. Biomed.* **6**, 317–323 (2002).

[76] Flynn, C. and McCormack, B. A. O., *Skin Research Technol.* **14**, 261–269 (2008).
[77] Flynn, C. O. and McCormack, B. A. O., *Comput. Meth. Biomech. Biomed. Eng.* **12**, 125–134 (2009).
[78] Kuwazuru, O., Saothong, J., and Yoshikawa, N., *Med. Eng. Phys.* **30**, 516–522 (2008).
[79] Roop, R. V., Plaut, R. H., Dillard, D. A., and Ohanehi, D. C., Peeling pressure-sensitive adhesive tape from initially-slack thin solid-film, *Proceedings of the 25th Annual Meeting of the Adhesion Society and the Second World Congress on Adhesion and Related Phenomena (WCARP-II)*, (Orlando, Florida, 2002), pp. 129–131.
[80] Plaut, R. H., *J. Adhesion* **86**, 675–697 (2010).
[81] Coffin, D. W. and Bloom, F., *Int. J. Non-Lin. Mech.* **34**, 935–947 (1999).
[82] Fried, I., *Computer Meth. Appl. Mech. Eng.* **49**, 163–173 (1985).
[83] Wolfram, S., *Mathematica: A System for Doing Mathematics by Computer*, (Addison-Wesley, Reading, Massachusetts, 1991).
[84] Lin, Y. Y., Hui, C. Y., and Wang, Y. C., *J. Polym. Sci. B: Polym. Phys.* **40**, 2277–2291 (2002).
[85] Zhang, L. and Wang, J., *Int. J. Adhesion Adhesives* **29**, 217–224 (2009).
[86] Wei, Y. and Hutchinson, J. W., *Int. J. Frac.* **93**, 315–333 (1998).
[87] Satas, D., Peel, in *Handbook of Pressure Sensitive Adhesive Technology*, 3rd ed., D. Satas (Ed.) (Satas and Associates, Warwick, Rhode Island, 1999), pp. 62–86.
[88] Aubrey, D. W., Welding, G. N., and Wong, T., *J. Applied Polymer Sci.* **13**, 2193–2207 (1969).
[89] Dahlquist, C. A., Pressure-sensitive adhesives, in *Treatise on Adhesion and Adhesives*, R. L. Patrick (Ed.) (Marcel Dekker, New York, 1969), Vol. 2, pp. 219–260.
[90] Kaelble, D. H., Theory and analysis of peel adhesion, in *Handbook of Pressure Sensitive Adhesive Technology*, 3rd ed., D. Satas (Ed.) (Satas and Associates, Warwick, Rhode Island, 1999), pp. 87–120.
[91] Bryant, R. A., *Am. J. Nursing* **88**, 189–190 (1988).
[92] Majidi, C., *Mech. Res. Comm.* **34**, 85–90 (2007).
[93] Kinloch, A. J. and Williams, J. G., The mechanics of peel tests, in *The Mechanics of Adhesion*, D. A. Dillard and A. V. Pocius (Eds.) (Elsevier, Amsterdam, 2002), pp. 273–301.
[94] Hamed, G. R. and Preechatiwong, W., *J. Adhesion* **79**, 327–348 (2003).
[95] Wilhelmi, B. J., Blackwell, S. J., Mancoll, J. S., and Phillips, L. G., *Ann. Plastic Surgery* **41**, 215–219 (1998).
[96] Christensen, S. F. and McKinley, G. H., *Int. J. Adhesion Adhesives* **18**, 333–343 (1998).
[97] Belhouari, M., Gouasmi, S., Bouiadjra, B. B., Achour, T., and Amiri, A., *Computat. Mater. Sci.* **44**, 835–837 (2008).
[98] Zhao, H. F., Chen, M., and Jin, Y., *Mater. Des.* **30**, 154–159 (2009).
[99] Song, J., Jiang, H., Huang, Y., and Rogers, J. A., *J. Vac. Sci. Technol. A* **27**, 1107–1125 (2009).
[100] Majidi, C. and Adams, G. G., *Mech. Res. Comm.* **37**, 214–218 (2010).
[101] Instron Corporation, *Application Report* (2006). Online: http://www.instron.com/wa/library/StreamFile.aspx?doc=1297
[102] Ciccotti, M., Giorgini, B., Vallet, D., and Barquins, M., *Int. J. Adhesion Adhesives* **24**, 143–151 (2004).
[103] Renvoise, J., Burlot, D., Marin, G., and Derail, C., *J. Adhesion* **83**, 403–416 (2007).